Journal of Inflammation Research

Dovepress
open access to scientific and medical research

Open Access Full Text Article

ORIGINAL RESEARCH

C/EBPβ Promotes LPS-Induced IL-1β Transcription and Secretion in Alveolar Macrophages via NOD2 Signaling

Yalan Luo[1–3,*], Peng Ge[1–3,*], Haiyun Wen[1–3,*], Yibo Zhang[1–3], Jin Liu[1,3], Xuanchi Dong[1,3], Bowen Lan[1,3], Guixin Zhang[1–3], Qi Yang[4], Hailong Chen[1–3]

[1]Laboratory of Integrative Medicine, The First Affiliated Hospital of Dalian Medical University, Dalian, People's Republic of China; [2]Institute (College) of Integrative Medicine, Dalian Medical University, Dalian, People's Republic of China; [3]Department of General Surgery, The First Affiliated Hospital of Dalian Medical University, Dalian, People's Republic of China; [4]Department of Traditional Chinese Medicine, The Second Affiliated Hospital of Dalian Medical University, Dalian, People's Republic of China

*These authors contributed equally to this work

Correspondence: Qi Yang; Hailong Chen, Email dyeyyq1016@163.com; chenhailong@dmu.edu.cn

Objective: C/EBPβ, a crucial transcription factor, regulates innate immunity and inflammatory responses. However, the role played by C/EBPβ in alveolar macrophage (AM) inflammatory responses remains unknown. This study aimed to investigate the role and mechanism of C/EBPβ in alveolar macrophages (AMs) from the transcriptional level and to search for natural compounds targeting C/EBPβ.

Methods: Rat AMs were infected with Lv-sh-C/EBPβ and treated with LPS, and the expression levels of iNOS, TNF-α, IL-6, and IL-1β were measured by RT-qPCR, Western blotting, and ELISA. Mechanistically, transcriptome sequencing (RNA-seq) revealed changes in gene expression patterns in AMs after LPS stimulation and C/EBPβ knockdown. Functional enrichment analyses and rescue experiments identified and validated inflammation-associated cell signaling pathways regulated by C/EBPβ. Furthermore, virtual screening was used to search for natural compounds that inhibit C/EBPβ with the structure of helenalin as a reference.

Results: Following stimulation with LPS, AMs exhibited an increased expression of C/EBPβ. C/EBPβ knockdown significantly decreased the expression levels of inflammatory mediators. A total of 374 differentially expressed genes (DEGs) were identified between LPS-stimulated C/EBPβ knockdown and negative control cells. The NOD-like receptor signaling may be a key target for C/EBPβ, according to functional enrichment analyses of the DEGs. Further experiments showed that the muramyl dipeptide (MDP, NOD2 agonist) reversed the downregulation of inflammatory mediators and the NF-κB pathway caused by the C/EBPβ knockdown. The virtual screening revealed that N-caffeoyltryptophan, orilotimod, and petasiphenone have comparable pharmacological properties to helenalin (a known C/EBPβ inhibitor) and demonstrate a great binding capacity to C/EBPβ.

Conclusion: Ablation of C/EBPβ may attenuate LPS-induced inflammatory damage in AMs by inhibiting the NOD2 receptor signaling pathway. Three natural compounds, N-caffeoyltryptophan, orilotimod, and petasiphenone, may be potential C/EBPβ inhibitors.

Keywords: C/EBPβ, alveolar macrophage, RNA-seq, NOD-like receptor signaling pathway, IL-1β, virtual screening

Introduction

Alveolar macrophages (AMs) are alveolar compartment resident phagocytes, constituting more than 90% of lung macrophages, with the ability to self-renew and serve as the first line of defense against extra-alveolar stimuli.[1] Under physiological conditions, AMs play a vital role in maintaining host defense and immune homeostasis in the lung by acting as sentinels to monitor and engulf foreign pathogens and senescent cells.[2] However, in response to stimulation by various pathogenic factors, AMs are excessively activated, which is thought to be the initiating factor of inflammatory damage in the lung.[3] Inflammation induction and recovery phases are accompanied by the explosive accumulation of macrophages in the lungs.

Received: 17 June 2022
Accepted: 1 September 2022
Published: 11 September 2022

Graphical Abstract

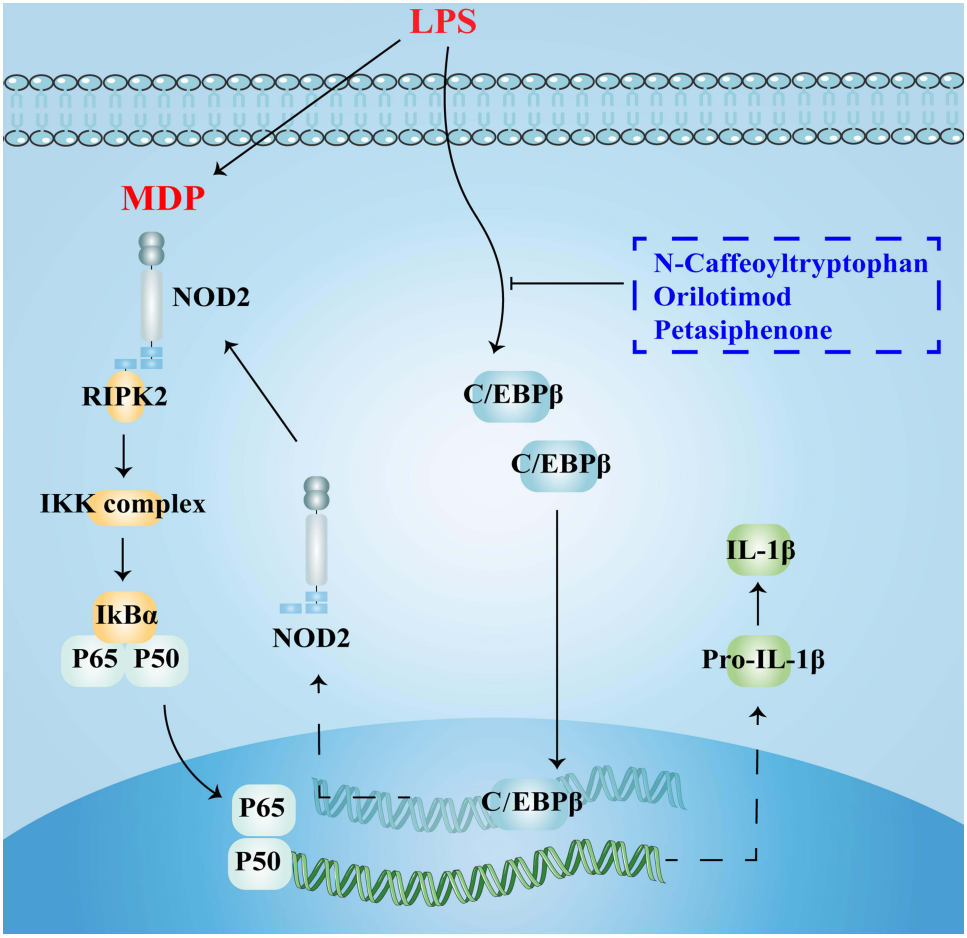

They synthesize and secrete a broad series of inflammation-inducing mediators, including the interleukins (ILs) family (IL-1β, IL-12, IL-23), TNF-α, chemokine family, inducible nitric oxide synthase (iNOS), which act as chemoattractants for invading cells (polymorphonuclear leukocytes), triggering an inflammatory cascade and a pro-inflammatory environment, causing inflammatory tissue damage.[4] Inflammatory mediators are effectors and magnifiers of macrophage-induced tissue injury, and inhibiting their expression and secretion is a powerful measure to attenuate organ damage. Unfortunately, transcriptional regulatory networks of inflammatory mediator expression in AMs have not yet been fully elucidated.

CCAAT enhancer binding protein β (C/EBPβ) is a transcription factor belonging to the basic leucine zipper (b-ZIP) family. In 1990, it was identified as a trans-acting factor that binds to the IL-1-responsive element in the IL-6 promoter.[5] Subsequent studies uncovered the presence of functional C/EBPβ binding sites in promoters of a series of genes, such as *fos*,[6] *mat1a*,[7] *ubqln4*,[8] *gas5*,[9] *tfam*,[10] *wee1*,[11] *c-myc*, and *il-4*.[12] C/EBPβ plays a vital role in regulating immune and inflammatory responses. Matsuda et al[13] demonstrated that C/EBPβ accumulation induced a loss of β-cell mass and insulin secretion. The rationale for the phenomena is that C/EBPβ accumulation blocked ATF6-mediated GRP78 transcription, making cells more susceptible to endoplasmic reticulum stress and eventually contributing to diabetes development. Chen et al[14] proposed that IL-7-induced bone marrow (BM) B-cell generation necessitates C/EBPβ. In C/EBPβ-/- mice, the expression level and bioactivity of IL-7 were decreased, and BM B cell expansion was impaired with reduced number and dysfunction. Apart from lymphocytes, evidence for the role of the C/EBPβ in macrophages rapidly

increases. Transcription of the C/EBPβ gene significantly increases in macrophages stimulated with M1-like stimuli.[15] Furthermore, the expression of C/EBPβ is closely related to macrophage inflammation.

In this study, we established a stable LPS-induced AM inflammation model, utilized loss of function experiments and RNA-seq technology to resolve the possible regulatory mechanisms of C/EBPβ in AM inflammation at the transcriptional level. We searched for natural compounds targeting C/EBPβ through virtual screening to provide an experimental basis and theoretical rationale for future treatment of lung inflammation by targeting C/EBPβ to inhibit AMs.

Materials and Methods

Packaging of Recombinant Lentivirus and Generation of Stably Transfected Cell Line

Three siRNA sequences targeting the rat C/EBPβ gene and a negative control scrambled sequence not matching any known gene were designed, and their corresponding short hairpin structure sequences (designated as sh-C/EBPβ and sh-NC) were synthesized by GeneChem (Shanghai, China). Sequences for relevant gene knockdown were listed in Supplementary Table 1. The sh-C/EBPβ and sh-NC sequences, respectively, were cloned into the hU6-MCS-CBh-gcGFP-IRES-puromycin plasmid vector. The sequence-validated recombinant plasmids were amplified in E. coli, and EndoFree Maxi Plasmid Kit (Tiangen Biotech Co., Ltd., Beijing, China) was adopted for plasmid extraction. The resulting recombinant plasmids and Lentivirus Package plasmid mix (GeneChem, Shanghai, China) were co-transfected into 293T cells (the Cell Bank of Chinese Academy of Sciences, Shanghai, China) with Lipofectamine™ 3000 (Invitrogen). After 72 h, 293T cells were harvested and broken to obtain lysate supernatants containing lentivirus particles. After column purification and gradient dilution, high titers packaged lentivirus particles (designated as Lv-sh-C/EBPβ and Lv-sh-NC) were obtained. NR8383 cells were infected with lentivirus at an MOI of 60. All cells were infected using transfection reagents HitransG P (GeneChem, Shanghai, China) and then treated with puromycin (Takara Bio Inc., Japan, 8 μg/mL) for 2–3 weeks to generate stable C/EBPβ-knockdown and negative control NR8383 cells.

Cell Culture and Study Design

The rat AM cell line NR8383 was purchased from Procell Life Science & Technology Co.,Ltd (Wuhan, China), and passages 2 to 8 were used for experiments. Cells were cultured in Ham's F-12K (Kaighn's) medium (Cat#10025, Macgene) supplemented with 20% fetal bovine serum (FBS, Gibico, NY, USA) and 1% penicillin/streptomycin. Prior to any experiment, cells were synchronized in G1/G0 phase via starvation in a serum-free medium for 2 days. The cells were divided into 5 groups: control (CON), lipopolysaccharide (LPS), LPS + Lv-sh-NC, LPS + Lv-sh-C/EBPβ, and LPS + Lv-sh-C/EBPβ + muramyl dipeptide (MDP). MDP is a bacterial cell wall component that is a NOD2 receptor agonist.[16] In brief, normal NR8383 cells and previously constructed stable C/EBPβ-knockdown and negative control NR8383 cells were seeded in 6-well plates. The cells were incubated overnight at 37°C for 24 hours in a CO_2 incubator. Stimulation was performed in triplicate for 24 h with LPS (200 ng/mL, from Escherichia coli 0127: B8, Cat#L4516, Sigma-Aldrich) or MDP (10 μg/mL, InvivoGen). Then, at times given, the supernatants and cells were taken for further experiments.

Western Blotting

The Whole Cell Lysis Kit and the BCA Protein Quantitation Kit (KeyGEN Bio TECH) were used to achieve cell protein extraction and quantification. Then Western blotting (WB) was performed according to a previously described standard method[17] using anti-C/EBPβ (1:1000, Cat#ab32358, Abcam), anti-iNOS (1:1000, Cat#OM641716, Omnimabs), anti-NOD2 (1:1000, Cat#A15992, ABclonal), anti-NOD1 (1:1000, Cat#DF6378, Affinity), anti-phospho-RIPK2 (1:500, Cat#AF0049, Affinity), anti-RIPK2 (1:1000, Cat#DF6967, Affinity), anti-phospho-NF-κB p65 (1:500, Cat#AP0123, ABclonal), anti-NF-κB p65 (1:1000, Cat#A16271, ABclonal), anti-IL-1β (1:1000, Cat#A1112, ABclonal), and anti-β-actin (1:20000, cat#AC026, ABclonal) antibodies. The experiments were independently performed in triplicate.

Table 1 The Sequences of Primers

Genes	Accession NO.	Type	Primer Sequence (5'–3')
il-1b	NM_031512	F	GGCAACTGTCCCTGAACTCAA
		R	GCTTCTCCACAGCCACAATGA
nod2	NM_001106172	F	GGCAGCACAGGTGGACTCTGAGGATA
		R	GCAGCAGCCTTAGCAGCAGTGAGTT
nod1	NM_001109236	F	CTCAAAGGAGGACCTGCTGCTGGA
		R	GAAGACAGTCTCGCCATGCTCGTTGA
il-17f	NM_001015011	F	CTGAGCGAAGAAGCAGCCATC
		R	CAACATCAACAGCAGCAGAGACT
gbp1	XM_017591353	F	GCAATATGGAAGTGTCATCTAACC
		R	AGAACCTCATCAGCCTGTAAG
herc6	NM_001012474	F	TCTGCTTAGAGGTCTTCCATACA
		R	AATGCCAGTGTCTTCCAGTTC
irf7	NM_001033691	F	TCTTTGACTTCAGCACTTTCTTCC
		R	AGGTAGATGGTGTAATGTGGTGAT
aim2	XM_039091426	F	TGTGGAGGTCACCAGTTCCT
		R	ACCTCCATGGTCCCTCTTTT
igf1	NM_178866	F	CACATCATGTCGTCTTCACACC
		R	GGAAGCAACACTCATCCACAATG
tyro3	NM_017092	F	GTGGAAGGAACTACGGCCAA
		R	GATGTACGGCTGTGAGGAGG
mmp12	NM_053963	F	CCCTGCATCTGTAAAGAAGATTGAT
		R	GCCTCACATCGTACCTCCAATATT
mmp3	NM_133523	F	TCCCAGGAAAATAGCTGAGAACTT
		R	GAAACCCAAATGCTTCAAAGACA
cxcl2	NM_053647	F	TCCTCAATGCTGTACTGGTC
		R	TGAAGTCAACCCTTGGTAGG
inos	NM_012611	F	GGATGTGGCTACCACTTTGA
		R	CATGATAACGTTTCTGGCTCTTG
cebpb	NM_001301715	F	GACACGGGACTGACGCAACAC
		R	CAACAACCCCGCAGGAACATCT
gapdh	NM_017008	F	GGCACAGTCAAGGCTGAGAATG
		R	ATGGTGGTGAAGACGCCAGTA

Reverse Transcription-Quantitative Polymerase Chain Reaction (RT-qPCR)

Total RNA was isolated from the different groups of NR8383 cells with *RNAex Pro* Reagent (Cat#AG21102, Accurate Biology, Hunan, China). Subsequently, 1 μg RNA of each sample was transcribed reversely into cDNA using the *Evo M-MLV* Reverse Transcription Mix Kit (Cat#AG11728, Accurate Biology). Synthesized cDNA served as the template of real-time quantitative PCR performed by SYBR® Green Premix *Pro Taq* HS qPCR Kit II (Cat#AG11702, Accurate Biology). PCR conditions are initial denaturation at 95°C for 30 s, 40 cycles of denaturation at 95°C for 5 s, annealing, and extension at 64°C for 30 s. The relative expression of target gene mRNA transcripts to the control GAPDH was quantified by the $2^{-\Delta\Delta CT}$ method.[18] The primers used are listed in Table 1. Each sample was run in triplicates.

Enzyme-Linked Immunosorbent Assay (ELISA)

The cytokines TNF-α (Cat#E-EL-R2856c, Elabscience, Wuhan, China), IL-6 (Cat#F15870, Westang Bio-tech Co., Ltd, Shanghai, China), and IL-1β (Cat#E-EL-R0012c, Elabscience, Wuhan, China) were secreted into the culture medium by AMs and measured with the ELISA kits.

RNA Extraction and High-Throughput Sequencing

Total RNA was extracted from cells using *RNAex Pro* Reagent. Then DNA digestion was carried out by DNaseI to purify RNA samples. The RNA concentration of each sample was determined through a SimpliNano spectrophotometer (GE Healthcare, US), with the OD260/OD280 and OD260/OD230 ratios as indicators of RNA purity. RNA integrity was viewed using 1.5% agarose gel electrophoresis. For quality control, the RNA sample had to meet the requirement of OD260/280 = 1.8 ~ 2.2 and OD260/230 ≥ 2.0.

The preparation of high-throughput RNA sequencing and deep sequencing were conducted by Ruixing Biotechnology (Wuhan, China). Specifically, ribosomal RNA (rRNA) was removed from the RNA samples using RNase H. The resulting rRNA-depleted RNA samples were then fragmented and reverse transcribed into cDNA using the KCTM Stranded mRNA Library Prep Kit for Illumina (Cat#DR08402, Seqhealth Technology Co., LTD, Wuhan, China). The cDNA fragments were then subjected to the end repair process (including adding a single "A" base and 5' - terminal phosphorylation, followed by adapter ligation) and amplification to construct libraries for RNA-seq analysis. Quality control and quantification of the libraries were performed with the Agilent 2100 bioanalyzer and real-time quantitative PCR (qPCR). Qualified libraries used Illumina high throughput sequencing platform NovaSeq 6000 for paired-end sequencing with the PE150 model.

Raw Data Processing

The overall quality of the RNA-seq raw data was checked using the FASTX-Toolkit software (http://hannonlab.cshl.edu/fastx_toolkit/). After trimming the 3' adaptor and eliminating low-quality reads by Cutadapt software (https://cutadapt.readthedocs.org/), high-quality clean reads were aligned to the rat reference genome mRatBN7.2 using TopHat2 software (https://ccb.jhu.edu/software/tophat/). Then, FPKM (the number of expected fragments per kilobase of transcript per million fragments mapped), the expression matrix of mRNA, was obtained using Cuffdiff software (http://cole-trapnell-lab.github.io/cufflinks/) under the guidance of Ensembl gtf gene annotation file. Also, the expression matrix was analyzed with the DESeq2 package in R software, and fold change (FC), and *p*-value for DEGs based on FPKM was generated. Based on adjusted < 0.05 and $|\log_2 FC| > 1$, the filtering requirements were applied.

Bio-Functional Enrichment Analyses

Gene Ontology (GO) and Kyoto Encyclopedia of Genes Genomes (KEGG) pathway analysis were performed to understand the biological functions of DEGs. The results were visualized with clusterProfiler in R package. In addition, the enrichment scores (ES) of the "c2.cp.kegg.v7.5.symbols.gmt" genome from the Molecular Signatures Database (MSigDB) in each group were counted using Gene Set Enrichment Analysis (GSEA) software (4.1.0). A nominal *p*-value of <0.05 and an FDR q-value of <0.25 were used as the cutoff criteria.

Virtual Screening

Discovery Studio 4.5 (DS 4.5) is a molecular modeling platform for drug design, protein modeling, and optimization that we utilize in our research to conduct virtual screening of potential C/EBPβ inhibitors. The RCSB protein data bank is an open-access biomolecule repository that houses the crystal structure of C/EBPβ, the receptor protein employed in this study (1H89). In particular, the ZINC database,[19] which the Irwin lab maintains, is one of the most comprehensive repositories of commercial compounds available. It provides the natural product data resources required for this study to succeed.

For the first screening of inhibitors, the Libdock module provides a fast docking procedure.[20] As a known C/EBPβ inhibitor, helenalin was used as a reference molecule for the candidate compounds.[21] It was chosen to use the helenalin-C/EBPβ complex's binding pocket as a reference site for the virtual screening process. Following the initial structure-based screening, all compounds are ranked by Libdock score, and the top 20 compounds and helenalin are chosen for further exploration and testing. The absorption, distribution, metabolism, and excretion (ADME) module tested the pharmacological properties of each of the 20 compounds and helenalin. Another source of concern is the issue of safety. The potential toxicity of the compounds was evaluated using the TOPKAT module. The final natural inhibitors were selected based on their pharmacological qualities listed above. It is utilized in conjunction with the CDOCKER module, which produces highly accurate molecular docking findings using the CHARMM force field[22] to calculate the interaction

and CHARMM energy of acceptor-ligand complexes, thus determining the best posture. The pharmacophore models generated by the feature mapping module are used to assess the candidate compounds' attribute elements. Finally, the optimal conformation of the acceptor-ligand complexes was imported, and molecular dynamics simulations were performed. Li's past study was the basis for the operational technique.[23]

Statistical Analysis

Data obtained from this study were presented as Mean ± Standard Error of the Mean. One-way analysis of variance (ANOVA) was used to compare means among multiple groups. Post Hoc Test was estimated using Fisher's Least Square Difference (LSD) or Tamhane based on the homogeneity of variance. P-value < 0.05 level was considered to be significant. Statistical analysis and visualization were performed using SPSS 24.0 and GraphPad Prism 8.0.

Results

C/EBPβ Knockdown Suppresses the LPS-Induced Inflammatory Cytokine Release in Alveolar Macrophages

Our experiments showed that C/EBPβ mRNA and protein expression were elevated in AMs treated with 200 ng/mL LPS. Loss-of-function experiments were performed further to investigate the role of C/EBPβ in AM inflammatory responses. First, three sh-RNA sequences were designed to achieve knockdown of C/EBPβ. It was found that the mRNA levels of C/EBPβ were significantly decreased in cells transfected with sh-RNA (sh-C/EBPβ#1, sh-C/EBPβ#2, and sh-C/EBPβ#3) compared to those transfected with sh-NC, and sh-C/EBPβ#3 had the best knockdown effect and was continued to be used for subsequent experiments (Supplementary Figure 1). Following that, we reduced C/EBPβ expression via sh-C/EBPβ transfection in LPS-treated NR8383 cells (Figure 1A and E). Then it was found that the levels of inflammatory cytokines (IL-6, TNF-α, IL-1β) secreted by the cells into the culture supernatant were significantly reduced after C/EBPβ knockdown (Figure 1B–D). Similarly, depletion of C/EBPβ also decreased the mRNA and protein levels of iNOS and IL-1β (Figure 1E–G). These findings showed that C/EBPβ is involved in the inflammatory response in LPS-stimulated AMs and that C/EBPβ downregulation may protect against it.

C/EBPβ Affects Expression Patterns of Inflammation-Related Genes in Alveolar Macrophages Treated with LPS

To reveal the mechanism of C/EBPβ regulation of AM inflammatory responses, we treated Lv-sh-NC or Lv-sh-C/EBPβ-infected AMs with LPS, respectively (Figure 2A), and performed a high-throughput RNA-seq analysis (Figure 2B). When comparing the LPS group to the control, a total of 1956 genes with statistically significant changes were discovered, 793 upregulated and 1163 downregulated (Figure 2C). 374 differentially expressed genes (DEGs) were identified in the LPS + sh-C/EBPβ group relative to the LPS + sh-NC group. Among them, 266 were upregulated, and 108 were downregulated (Figure 2D). Interestingly, transcriptome analysis showed that C/EBPβ depletion resulted in significant upregulation of several anti-inflammatory mediators (TYRO3 and IGF1) capable of driving macrophage polarization to M2 type and downregulation of several pro-inflammatory mediators, including matrix metalloproteinase 12 (MMP12), MMP3, and absent in melanoma 2 (AIM2). Besides, C/EBPβ also altered the expression of genes associated with macrophage chemotaxis (CXCL2 and IL-17F) and some interferon-inducible genes (IRF7, HERC6, and GBP1). Subsequently, the genes mentioned above, all associated with inflammatory response and cytokine release, were selected to verify the RNA-seq data by RT-qPCR. MMP12, MMP3, AIM2, CXCL2, IL-17F, IRF7, HERC6, and GBP1 expression levels were considerably raised in the LPS group and decreased by C/EBPβ knockdown, as seen in Figure 2E. In contrast, TYRO3 and IGF1 were downregulated in the LPS group and elevated after C/EBPβ interference. These findings support the reliability of the RNA-seq results and the role of C/EBPβ in the transcriptional regulation of inflammation-related genes.

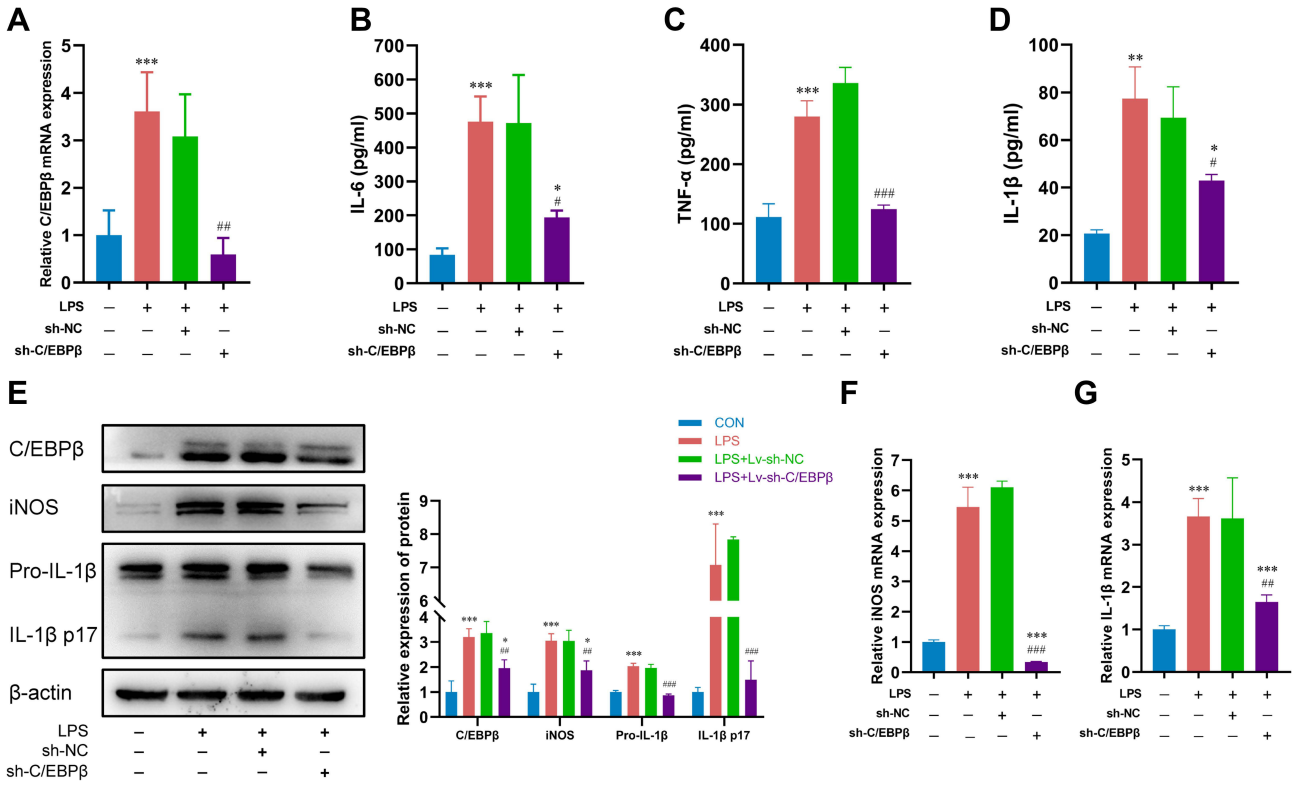

Figure 1 Depletion of C/EBPβ led to recovery from LPS-induced inflammatory injury in alveolar macrophages. (**A**) RT-qPCR was utilized to detect C/EBPβ mRNA level in LPS-treated NR8383 cells transfected with sh-C/EBPβ. (**B**–**D**) Levels of pro-inflammatory factors IL-6, TNF-α and IL-1β were assessed utilizing commercial assay kits in NR8383 cells. (**E**) The protein levels of C/EBPβ, iNOS and IL-1β were measured by Western blotting. (**F** and **G**) Transfected with sh-NC or sh-C/EBPβ, NR8383 cells treated by LPS underwent RT-qPCR analysis for iNOS and IL-1β expression. $^{*}p < 0.05$, $^{**}p < 0.01$, and $^{***}p < 0.001$ compared with the CON group. $^{\#}p < 0.05$, $^{\#\#}p < 0.01$, and $^{\#\#\#}p < 0.001$ compared with the LPS + sh-NC group.

Bio-Functional Enrichment Analyses

First, the DEGs were analyzed using GO and KEGG pathways to investigate the effects of LPS stimulation and C/EBPβ knockdown on AMs. As shown in Figure 3A, DEGs between the LPS and CON groups were significantly enriched in multiple GO terms, including response to lipopolysaccharide, inflammatory response, response to drug, and positive regulation of chemokine production. KEGG pathway analysis revealed that DEGs between the LPS and CON groups were significantly enriched in TNF, NOD-like receptor, and Toll-like receptor signaling pathways (Figure 3B). Similarly, DEGs identified between the LPS + Lv-sh-C/EBPβ and LPS + Lv-sh-NC groups were highly enriched in the GO biological process in terms of metabolic process, oxidation-reduction process, peptidyl-serine phosphorylation, calcium ion transport, response to organic cyclic compound and immune response (Figure 3C). And the enriched KEGG pathways included those referred to as alanine, aspartate, and glutamate metabolism, glutathione metabolism, purine metabolism, and cAMP signaling pathway, among others (Figure 3D). GO and KEGG analyses are the most widely used and accepted functional enrichment methods. However they still have some limitations, focusing mainly on DEGs while disregarding genes that vary but are not statistically significant. To more comprehensively investigate the impact of C/EBPβ downregulation on AM function, we further conducted GSEA using the LPS + Lv-sh-C/EBPβ and LPS + Lv-sh-NC expression data sets to uncover signaling pathways that C/EBPβ differentially activates. GSEA showed that gene sets related to NOD-like receptors and JAK/STAT signaling pathways were significantly ($q < 0.25$) downregulated in C/EBPβ deficiency (Figure 3E and F). Given the above findings, the pro-inflammatory effects of C/EBPβ on AM inflammation may be linked to the NOD-like receptor signaling pathway.

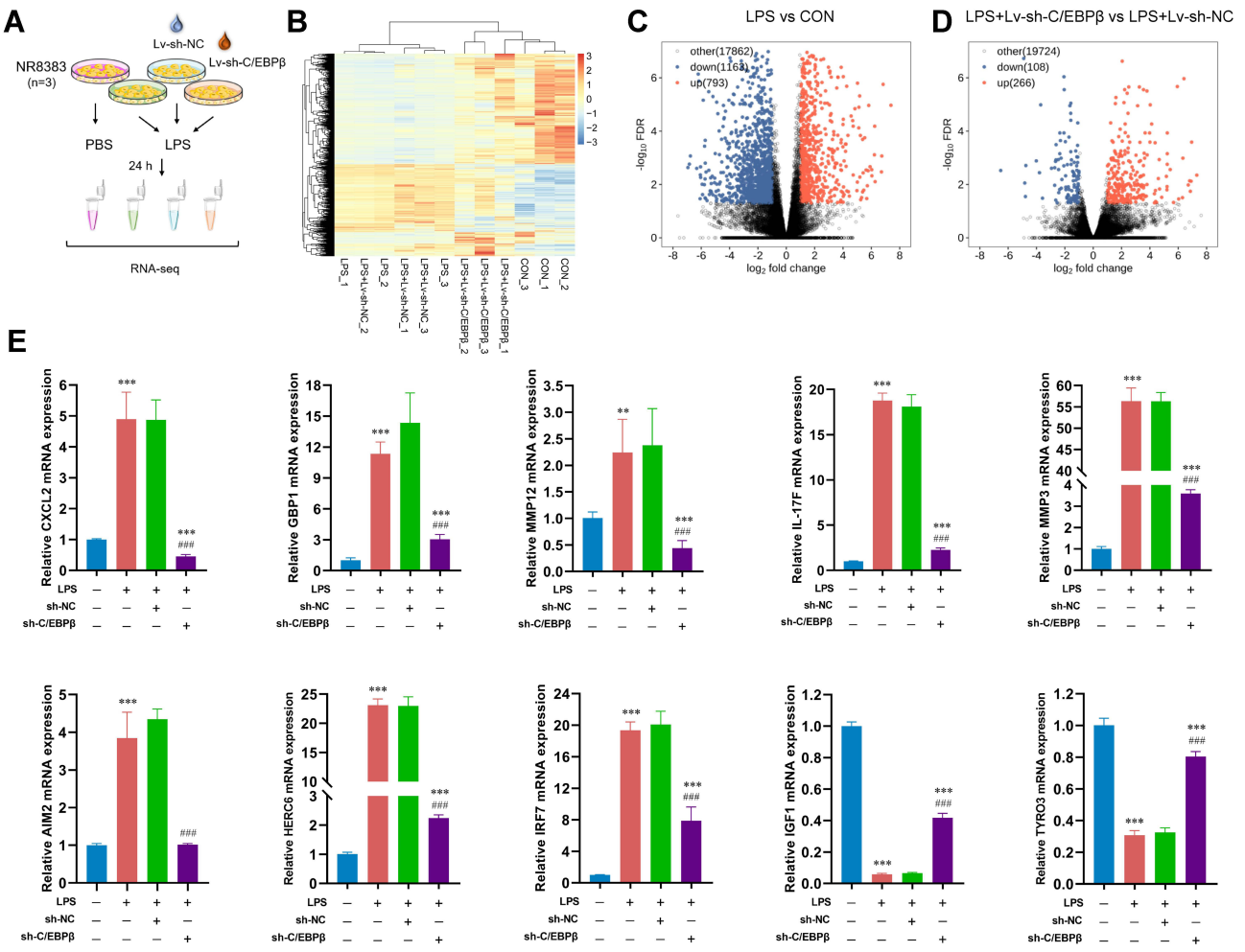

Figure 2 RNA-seq analysis of DEGs after C/EBPβ inhibition. (**A**) Flow chart of sample preparation for RNA-seq. (**B**) Heat maps of differentially expressed genes (DEGs). (**C**) Volcano plot indicating substantial changes in gene expression between the LPS and CON groups (up) and (down). (**D**) Volcano plot indicating substantial changes in gene expression between the LPS + Lv-sh-C/EBPβ and LPS + Lv-sh-NC groups (up) and (down). (**E**) Validation of C/EBPβ-regulated DEGs in alveolar macrophages using RT-qPCR. $^{**}p < 0.01$, and $^{***}p < 0.001$ compared with the CON group. $^{\#\#\#}p < 0.001$ compared with the LPS + sh-NC group.

C/EBPβ Mediates IL-1β Expression Through the NOD2/RIPK2/NF-κB Pathway in Alveolar Macrophages

We used RT-qPCR and Western blotting to examine NOD1 and NOD2 receptor expression levels to corroborate the findings of RNA-seq and functional enrichment analyses. mRNA and protein expression of NOD1 and NOD2 were markedly increased in AMs treated with LPS. The knockdown of C/EBPβ dramatically reduced NOD2 mRNA and protein expression. However, the NOD1 level showed no significant change (Figure 4A–C). This suggests that the regulatory effect of C/EBPβ on IL-1β may depend on NOD2 rather than NOD1. Next, we performed rescue experiments using MDP to further test whether C/EBPβ-mediated IL-1β synthesis and release through regulating the NOD2 signaling pathway. The mRNA expression of NOD2 and IL-1β in NR8383 cells was increased by the treatment with MDP (Supplementary Figure 2). As expected, after MDP was used in C/EBPβ-deficient AMs stimulated by LPS, the accumulation of NOD2 partially restored the IL-1β level (Figure 4D–F). Similarly, activation of the NOD2 receptor counteracted the downregulation in the protein expression of p-RIPK2, p-NF-κB, pro-IL-1β, and active IL-1β p17 by C/EBPβ knockdown (Figure 4G and H). Together, these data provide robust evidence that C/EBPβ contributes to the IL-1β transcription and secretion in AMs through the NOD2/RIPK2/NF-κB pathway.

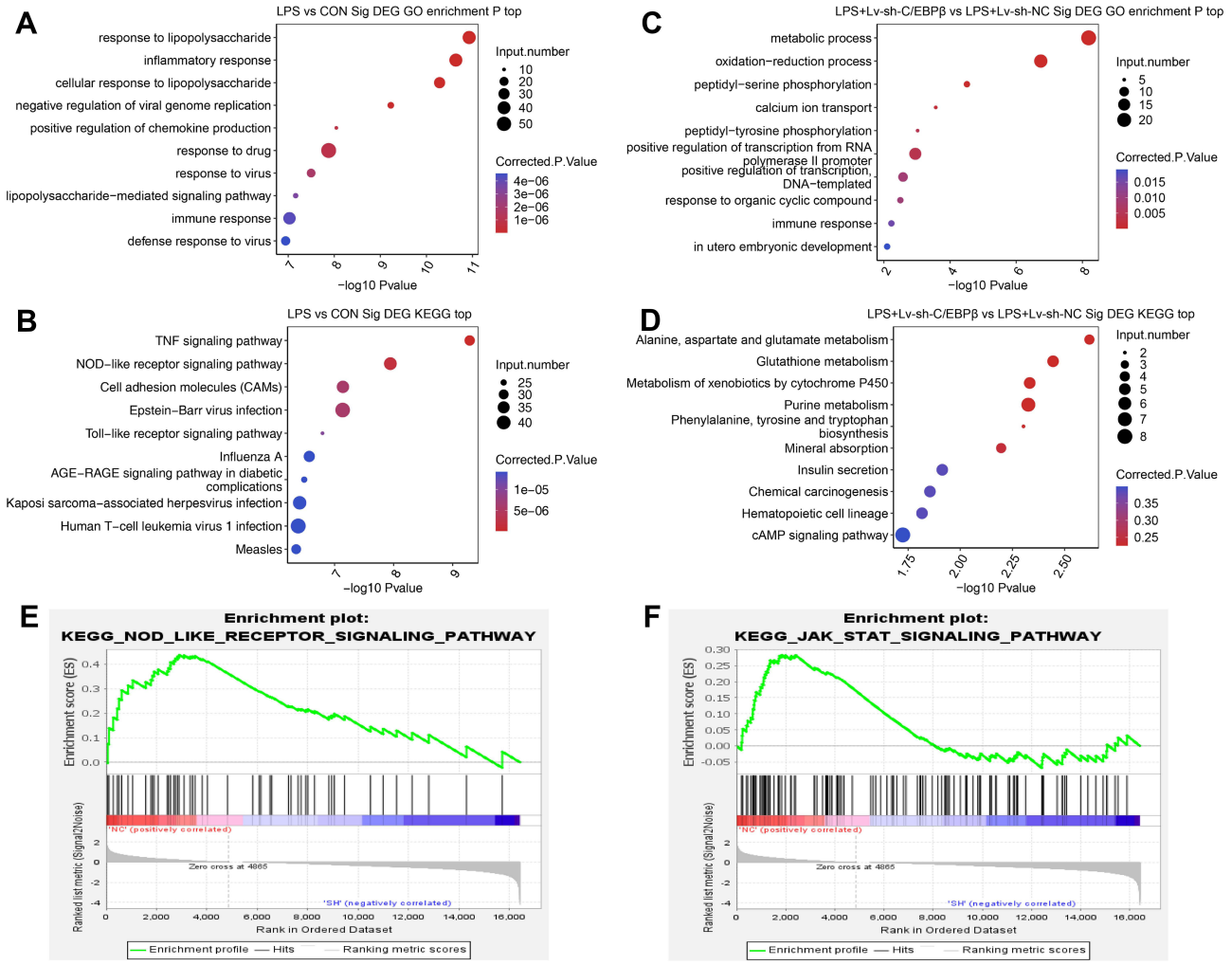

Figure 3 Functional enrichment analysis of DEGs. (**A** and **B**) Functional enrichment analysis showed the enriched biological processes and pathways of the DEGs between LPS and CON group. (**C** and **D**) GO and KEGG enrichment analysis showed the enriched biological processes and pathways of the DEGs between LPS + Lv-sh- C/EBPβ and LPS + Lv-sh-NC group. (**E** and **F**) GSEA showed that the NOD-like receptor and JAK/STAT signaling pathways are affected by C/EBPβ knockdown.

Virtual Screening Based on Libdock, ADME, and TOPKAT Modules

To find C/EBPβ inhibitors, we used the helenalin-C/EBPβ complex binding pocket as a reference. The docking activity of 14,926 natural compounds, including helenalin, with C/EBPβ, was thoroughly studied using the Libdock module. The top 20 compounds were chosen according to their scores, which were all above helenalin's (84.38), as shown in Table 2. Along with binding activity, the pharmacological features of natural compounds, such as solubility, human intestinal absorption, blood-brain barrier (BBB), cytochrome P450 2D6 (CYP2D6) binding, plasma protein binding levels (PPB), and hepatotoxicity, are critical criteria for virtual screening. We determined the ADME parameters for 20 natural compounds and helenalin using the ADME module. Table 3 shows that 11 natural compounds and helenalin are highly soluble in water. 13 compounds have a low or undefined BBB level. In terms of intestinal absorption level, 12 compounds perform as well as helenalin. Additionally, 7 compounds excluding helenalin were identified as potential CYP2D6 inhibitors. Hepatotoxicity was seen in 14 compounds and helenalin. As indicated in Table 4, the TOPKAT module estimated the potential toxicity of the compounds, including developmental toxicity potential (DTP), US National Toxicology Program rodent carcinogenicity (NTP), and Ames mutagenicity (AMES) properties. More specifically, all 20 compounds and helenalin tested were non-mutagen, with only 8

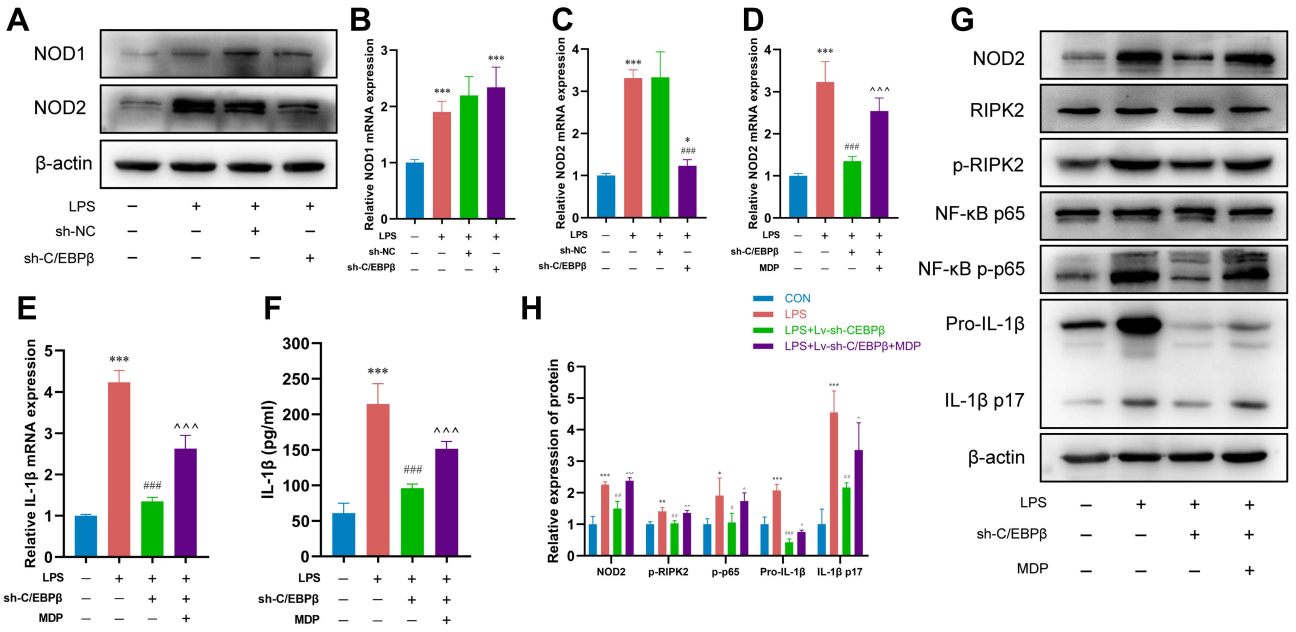

Figure 4 C/EBPβ targets the NOD2/RIPK2/NF-κB pathway to regulate IL-1β transcription and secretion. (**A**–**C**) The protein and mRNA levels of NOD1 and NOD2 were detected using WB and RT-qPCR in LPS-treated NR8383 cells transfected with sh-NC or sh-C/EBPβ. (**D**) The agonistic effect of MDP on NOD2 receptor was detected by RT-qPCR. (**E** and **F**) The level of IL-1β was detected via RT-qPCR and ELISA in response to sh-C/EBPβ or sh-C/EBPβ + MDP in LPS-induced NR8383 cells. (**G** and **H**) WB and its histogram were used to assess the expression levels of NOD2, RIPK2, p-RIPK2, NF-κB p65, NF-κB p-p65, Pro-IL-1β and IL-1β p17 in LPS-intoxicated NR8383 cells transfected with different plasmids. *$p < 0.05$, **$p < 0.01$, and ***$p < 0.001$ compared with the CON group. $^{\#}p < 0.05$, $^{\#\#}p < 0.01$, and $^{\#\#\#}p < 0.001$ compared with the LPS/LPS + sh-NC group. ^$p < 0.05$, ^^$p < 0.01$, ^^^$p < 0.001$ compared with the LPS + sh-C/EBPβ group.

compounds excluding helenalin testing negative for DTP. Furthermore, three compounds were anticipated to be non-carcinogenic in rodents.

As a result, we picked compounds ZINC000014824077, ZINC000014774634, and ZINC000004544883 as the potential inhibitors for the next round of the research.

Ligand Binding, Pharmacophore Analyses, and Molecular Dynamics Simulation

Following two screens, we used the CDOCKER module to explore the ligand-binding pattern of the three potential inhibitors and C/EBPβ. The ligand-receptor binding is more stable and affiliative when the interaction energy is lower. The interaction energy of the three potential inhibitors that we evaluated was lower than that of helenalin, indicating that all three potential inhibitors have a high affinity for C/EBPβ (Table 5). The hydrogen bonds (HBs) and π-related interactions between the potential inhibitors and C/EBPβ are depicted in Figure 5.

Table 2 The Libdock Scores of the Top 20 Compounds

NO.	Compounds	Libdock Score	NO.	Compounds	Libdock Score
1	ZINC000012958448	134.109	11	ZINC000000039452	127.777
2	ZINC000014819637	132.939	12	ZINC000014774634	127.658
3	ZINC000015115226	132.898	13	ZINC000013436567	127.195
4	ZINC000006094027	131.952	14	ZINC000003637160	127.016
5	ZINC000013412042	130.895	15	ZINC000004655405	126.748
6	ZINC000014763050	129.431	16	ZINC000004544883	126.606
7	ZINC000008220075	129.329	17	ZINC000004096962	126.584
8	ZINC000014824077	128.593	18	ZINC000019796031	125.427
9	ZINC000014762603	128.18	19	ZINC000001531449	125.347
10	ZINC000014947781	128.135	20	ZINC000043200202	125.24

Table 3 ADME of the Top 20 Compounds and Helenalin

Compounds	Solubility Level[a]	BBB Level[b]	CYP2D6[c]	Hepatotoxic[d]	Absorption Level[e]	PPB Level[f]
ZINC000012958448	4	4	0	1	3	0
ZINC000014819637	2	1	1	1	0	1
ZINC000015115226	2	1	1	1	0	1
ZINC000006094027	3	3	0	1	0	1
ZINC000013412042	2	4	0	1	1	1
ZINC000014763050	2	4	0	1	1	1
ZINC000008220075	3	4	0	1	3	0
ZINC000014824077	3	4	0	1	0	0
ZINC000014762603	2	4	1	1	1	1
ZINC000014947781	2	2	0	1	0	1
ZINC000000039452	2	2	1	1	0	0
ZINC000014774634	4	4	0	1	0	0
ZINC000013436567	3	4	0	1	3	0
ZINC000003637160	3	2	1	0	0	0
ZINC000004655405	3	1	1	0	0	1
ZINC000004544883	5	4	0	0	3	0
ZINC000004096962	4	4	0	0	3	0
ZINC000019796031	2	1	1	1	0	1
ZINC000001531449	2	1	0	0	0	1
ZINC000043200202	3	3	0	0	0	1
Helenalin	3	3	0	1	0	1

Notes: [a]0, Extremely low; 1, Very low, but possible; 2, Low; 3, Good; 4, Optimal; 5, Soluble. [b]0, Very high penetrant; 1, High; 2, Medium; 3, Low; 4, Undefined. [c]0, Non-inhibitor; 1, Inhibitor. [d]0, Nontoxic; 1, Toxic. [e]0, Good; 1, Moderate; 2, Low; 3, Very low. [f]0, Absorbent weak; 1, Absorbent strong.

The Feature Mapping module calculated the pharmacophores for the three possible ligands and helenalin. As illustrated in Figure 6, ZINC000014824077 exhibited 18 features, including 8 HB acceptors, 4 HB-donors, 2 hydrophobics, and 4 ring aromatics. 17 features in ZINC000004544883, including 8 HB acceptors, 2 HB-donors, 2 hydrophobics, one positive ion, and 4 ring aromatics. ZINC000014774634 exhibited 19 features, including 13 HB acceptors and 6 HB-donors. In addition, helenalin possessed 14 features, including 9 HB acceptors, 2 HB-donors, and 3 hydrophobics.

The last step was to run a simulation of the inhibitor-C/EBPβ complex in a realistic setting using the molecular dynamics simulation module. The complexes' CDOCKER potential energy and RMSD curves were determined. Figure 7 depicts how the complex's potential energy and RMSD progressively stabilized. As a result, ZINC000014824077, ZINC000014774634, and ZINC000004544883 are capable of interacting with C/EBPβ and remaining stable in normal environments.

Discussion

Pulmonary macrophages, which consist of AMs, interstitial, and bronchial macrophages, are the most significant immune cells in maintaining immunological homeostasis and host defense in the lung.[3] Among them, more than 90% of the pulmonary macrophages are AMs. Tissue-resident AMs in lung tissue and monocytes from bone marrow are the two primary sources of AMs. The tissue-resident AMs are adequate under physiological circumstances to sustain lung immunological homeostasis without supplementing circulating monocytes.[3] However, many circulating monocytes are attracted into lung tissue under pathological situations such as inflammation, injury, and infection, where they differentiate into AMs and polarize into macrophages with various functional phenotypes. Bronchoalveolar lavage fluid analysis showed that when the lungs were stimulated by inhaled particulates,[24] cigarette smoke,[25] pathogens,[26] or mechanical ventilation,[27] the total number of infiltrated AMs in the lung increased and polarized to the pro-inflammatory phenotype, releasing a large number of inflammatory mediators and initiating an inflammatory reaction. Influenced by environmental triggers, the role of AMs has been defined differently, which is extremely malleable and

Table 4 Toxicity of the Top 20 Compounds and Helenalin

Compounds	Mouse NTP[a]		Rat NTP[a]		Ames[b]	DTP[c]
	Female	Male	Female	Male		
ZINC000003637160	0	0	0	0	0	1
ZINC000014774634	0	0	0	0	0	0
ZINC000006094027	0	0	0	0	0	1
ZINC000013412042	0	1	0	1	0	1
ZINC000012958448	0	0	0	1	0	1
ZINC000019796031	1	1	1	1	0	0
ZINC000004544883	0	0	1	0	0	0
ZINC000004655405	0	1	1	0	0	0
ZINC000000039452	0	0	1	0	0	1
ZINC000013436567	0	0	1	1	0	1
ZINC000014947781	0	1	1	0	0	0
ZINC000014763050	0	1	1	0	0	1
ZINC000008220075	0	0	1	1	0	0
ZINC000014819637	0	1	1	0	0	1
ZINC000015115226	0	1	1	0	0	1
ZINC000014824077	0	0	1	0	0	0
ZINC000004096962	0	0	1	0	0	1
ZINC000001531449	0	0	1	0	0	1
ZINC000043200202	0	1	1	0	0	0
ZINC000014762603	0	1	1	0	0	1
Helenalin	0	1	1	0	0	1

Notes: [a]0, Non-carcinogen; 1, Carcinogen. [b]0, Non-mutagen; 1, Mutagen. [c]0, Nontoxic; 1, Toxic.

Table 5 CDOCKER Interaction Energy of Inhibitors with C/EBPβ

Compounds	-CDOCKER Interaction Energy (Kcal/mol)
ZINC000014824077	50.1275
ZINC000004544883	56.0862
ZINC000014774634	37.1494
Helenalin	30.3718

heterogeneous. AM polarisation and pro-inflammatory phenotype switching are closely associated with the balance of pulmonary inflammatory microenvironment.[28] Therefore, inhibition of excessive activation of AMs is considered a therapeutic target for ALI.

In C/EBPβ-deficient monocytes/macrophages, the expression of pathogen-associated molecular patterns (PAMPs) and/or supporting phagocytosis is significantly reduced. Antimicrobial genes (iNOS, lysozyme, hepcidin, and granulysin) were diminished, resulting in decreased macrophage phagocytosis.[29] Consistently with these findings, Tanaka et al[30] observed that C/EBPβ-/- mice are more vulnerable to Candida albicans, Listeria monocytogenes, and Salmonella typhimurium infections. These investigations indicate that C/EBPβ is essential for macrophage innate immunological activity. We anticipated that C/EBPβ also plays a non-negligible role in macrophage inflammation. Our research revealed the upregulation of several pro-inflammatory mediators of TNF-α, IL-1β, IL-6, and iNOS in LPS-treated AMs, and the knockdown of C/EBPβ effectively rectified these abnormalities. IL-1β, a versatile inflammatory cytokine, plays a crucial role in inflammation and immune response. Specifically, extracellular DAMPs and PAMPs trigger pattern recognition receptors such as toll-like receptors and NOD-like receptors (NLRs), which then activate inflammatory signaling pathways such as ERK-1/2 and NF-κB and enhance the synthesis of pro-IL-1β. Inflammasomes are intimately associated with IL-1β.[31] Firstly, inflammasomes enhance pro-caspase-1 hydrolysis. Caspase-1 then hydrolyzes pro-IL-1β into IL-1β by cleaving it. Notably, caspase-1 cleaves the Gasdermin

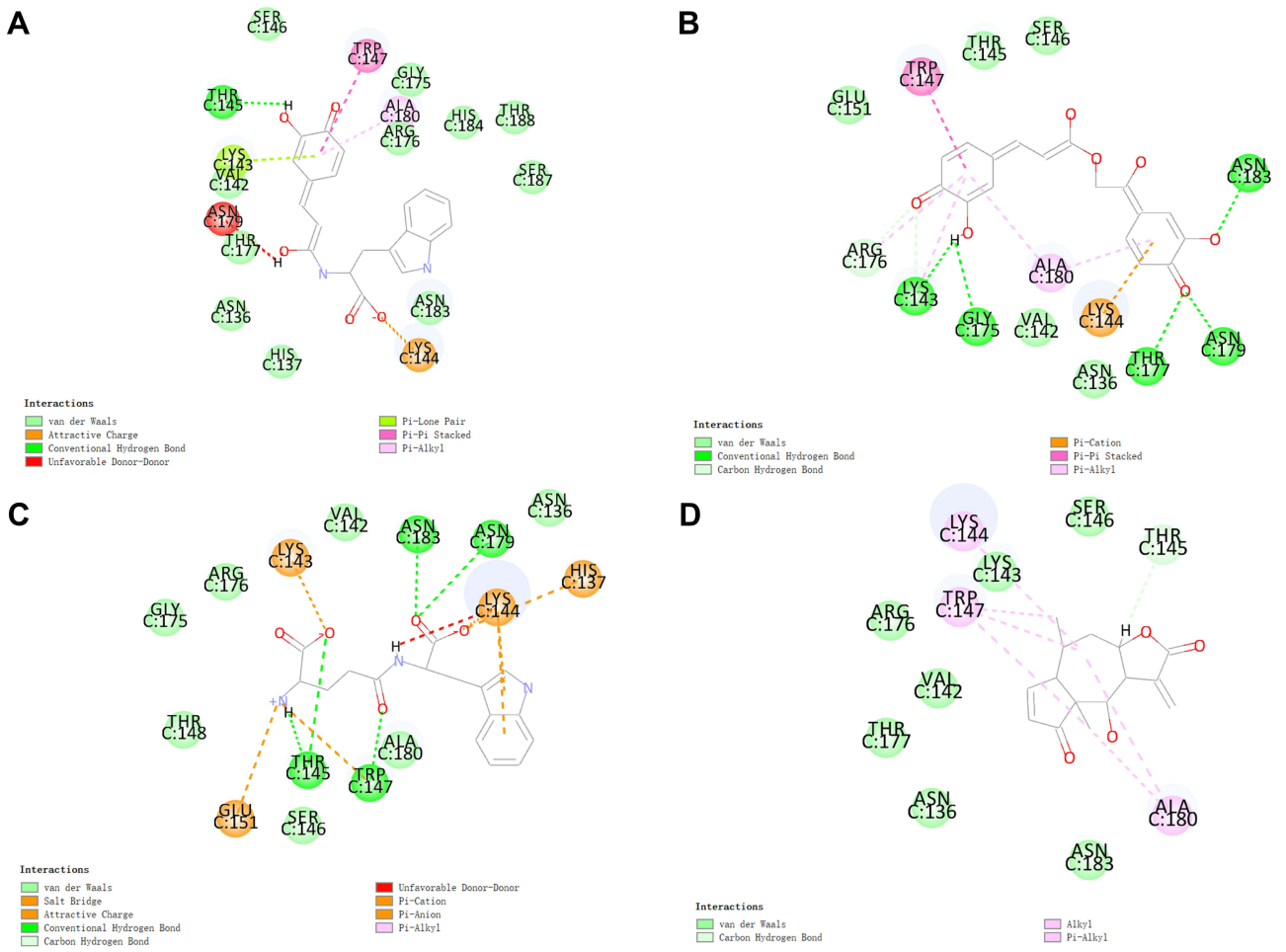

Figure 5 The predicted binding modes between C/EBPβ and (**A**) ZINC000014824077, (**B**) ZINC000014774634, (**C**) ZINC000004544883, and (**D**) Helenalin.

D protein to create the Gasdermin D N-terminal, which may cause the formation of holes in the cell membrane and the release of IL-1β. Monocytes/macrophages are the predominant cell type that secretes IL-1β. In pulmonary inflammatory diseases such as lung infection,[32] pulmonary fibrosis,[33] asthma,[34] and ALI,[35] a high number of IL-1β produced by AMs correlates strongly with disease severity. We found that iNOS and IL-1β mRNA and protein expression were extremely high in the LPS-treated AMs, and the knockdown of C/EBPβ significantly altered this phenomenon. Our findings imply that C/EBPβ promotes the IL-1β secretion and release of LPS-activated AMs. This is comparable to prior results. Ox-LDL stimulation increases C/EBPβ expression in THP-1 cells (human monocyte cell line), and C/EBPβ directly stimulates the release of several inflammatory cytokines, including IL-18 and IL-1β.[36] Consequently, we were intrigued by how C/EBPβ stimulates a high level of IL-1β secretion in AMs.

Our RNA-Seq data showed that LPS induces a substantial change in the gene expression profile of AMs, and a wide variety of functions, including the response to lipopolysaccharide, inflammatory response, and positive control of chemokine production, are connected to DEGs. When comparing the LPS + Lv-sh- C/EBPβ and LPS + Lv-sh-NC groups, we identified 374 DEGs. In addition, we validated 10 DEGs connected to macrophage inflammation. RT-qPCR analysis showed the trends of MMP12, MMP3, AIM2, chemokine (C-X-C motif) ligand 2 (CXCL2), IRF7, IL-17F, HERC6, GBP1, TYRO3, and IGF1 10 genes were consistent with the RNA-Seq results. Chemokine-mediated signaling is involved in monocyte macrophages and neutrophils' activation, recruitment, adhesion, and immune response. A typical chemokine generated by pro-inflammatory AMs, CXCL2, also known as macrophage inflammatory protein 2, increases lung inflammation by attracting and activating neutrophils.[37] A recent study revealed that CXCL2 affects the metabolic profile and phagocytic capacity of AMs. CXCL2 may be one of the markers to distinguish the heterogeneity of the AMs

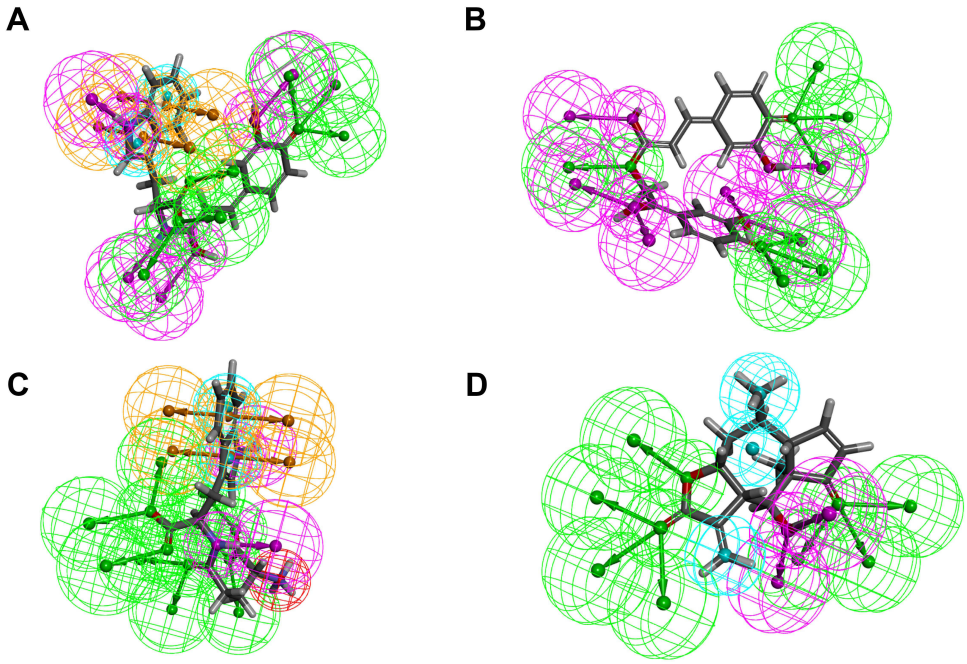

Figure 6 The pharmacophores of (**A**) ZINC000014824077, (**B**) ZINC000014774634, and (**C**) ZINC000004544883, and (**D**) Helenalin.

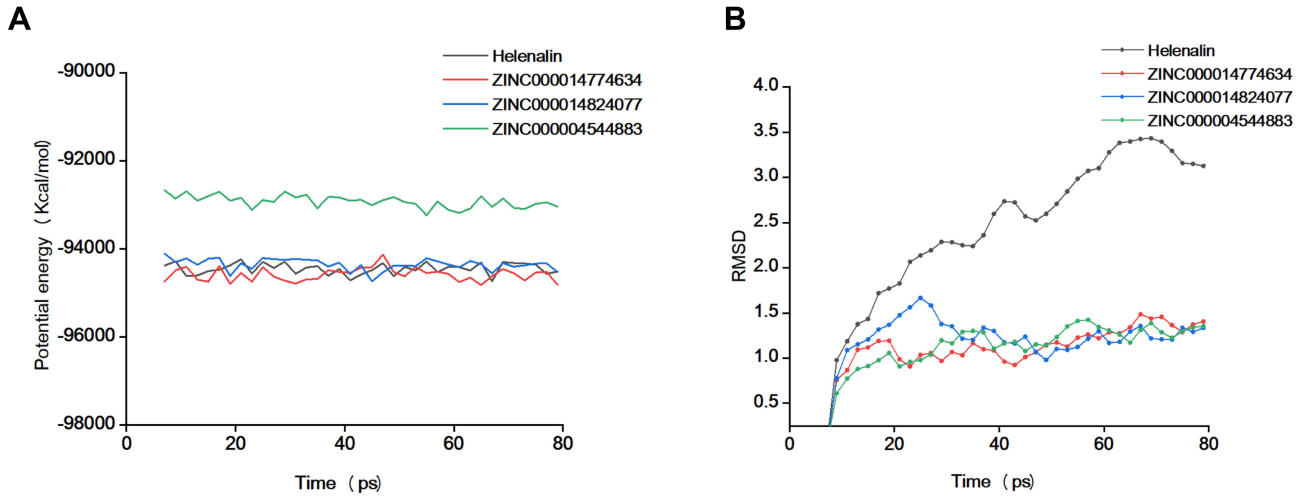

Figure 7 Molecular dynamics simulation of potential inhibitor-C/EBPβ complex. (**A**) Potential energy; (**B**) Root-mean-square deviation (RMSD).

population.[38] Our findings are in line with past research. AMs treated with LPS exhibited significantly elevated CXCL2 mRNA and inflammatory factors levels. Knockdown of C/EBPβ reversed the upregulation of CXCL2 by LPS.

AIM2 inflammasome, on par with NLRP3 inflammasome, promotes the release of cleaved IL-1β, leading to cell pyroptosis. Specifically, AIM2 inflammasome-mediated AM pyroptosis profoundly affects the progression of lung injury. IAV infection increased the expression of AIM2 in lung tissue and promoted IL-1β-mediated pyroptosis, according to the research of Zhang et al.[39] Several exciting experiments in vitro identified AIM2, which has macrophage-specific functions, as an essential mediator of the pro-inflammatory response exerted by IAV. In a word, an inflammatory response by AMs and AIM2 vesicles is linked. Another study found a link between silica and macrophage pyroptosis. They discovered that AIM2 activation is critical in silica's ability to stimulate lung immune cells.[40] We found that LPS increased AIM2 expression compared to the control group. C/EBPβ knockdown suppressed AIM2 transcription. This

suggests that C/EBPβ may exert pro-inflammatory effects by promoting AIM2 inflammasome-mediated pyroptosis. According to these findings, the data from RNA-seq are plausible.

Depletion of C/EBPβ led to a reduction in inflammatory responses in LPS-treated AMs through the regulation of the NOD-like receptor signaling pathway, according to enrichment analyses on DEGs. The innate immune response is triggered when NLRs, a subclass of pattern recognition receptors in the cytoplasm, detect damage-related molecular patterns. NLRs are the primary intracellular triggers of macrophage inflammatory and immunological responses.[41] We found that C/EBPβ may affect IL-1β synthesis and secretion by regulating NLRs transcription. And C/EBPβ promotes IL-1β secretion dependent on NOD2 but not NOD1, which is essential. NOD1 recognizes iE-DAP in Gram-negative bacteria, while NOD2 is able to recognize MDP, which is found in practically all bacterial cell walls. The majority of researchers are of the opinion that NOD1 is capable of a broader range of actions than NOD2. However, C/EBPβ knockdown significantly inhibits NOD2 mRNA and protein expression while not significantly regulating NOD1 expression. C/EBPβ knockdown was found to be counteracted by MDP therapy in subsequent rescue experiments. These data support the hypothesis that NOD2 may function as a critical cytoplasmic receptor for C/EBPβ in order to stimulate the transcription and secretion of IL-1β.

Computer-aided drug design tools, such as molecular docking and molecular dynamics simulation, have been increasingly popular in drug discovery in recent years. In light of C/EBPβ's function in LPS-induced AM inflammatory responses, we developed a structure-based virtual screening scheme for C/EBPβ inhibitors using helenalin as a reference structure. The Libdock results reveal that the ligands ZINC000014824077 (N-caffeoyltryptophan), ZINC000004544883 (orilotimod), and ZINC000014774634 (petasiphenone) bind C/EBPβ proteins better than helenalin. Furthermore, the three candidate compounds may be less harmful than helenalin, particularly because orilotimod is not hepatotoxic. The three compounds outperform helenalin according to DTP, NTP, and AMES tests. Compared to helenalin, they have lower carcinogenic potential. The CDOCKER data revealed that N-caffeoyltryptophan, orilotimod, and petasiphenone have lower potential energy than helenalin, indicating a higher binding affinity. Aside from that, molecular dynamics simulations indicated that the ligand-receptor complexes might maintain stability in the natural environment. As a result, the three candidate inhibitors identified through virtual screening exhibit high binding affinity and stability, providing fresh insights into the development of C/EBPβ inhibitors.

Our research demonstrates that C/EBPβ is highly increased in LPS-stimulated AMs and that knockdown of C/EBPβ suppresses transcription and translation of IL-1β via inhibiting the NOD2/RIPK2 signaling pathway, alleviating LPS-mediated inflammatory responses in AMs. Previous research has not identified these outcomes. We shed light on the novel mechanism by which LPS induces IL-1β secretion. Our findings provide a solid groundwork for follow-up studies. Furthermore, virtual screening found three natural compounds, including N-caffeoyltryptophan, orilotimod, and petasiphenone, as potential inhibitors of C/EBPβ. The severity of human inflammatory diseases such as pulmonary inflammation,[42] osteoarthritis,[43] neuroinflammation,[44] and liver inflammation[45] is well recognized as directly connected with IL-1β accumulation. Therefore, as selective inhibitors of C/EBPβ, which regulate IL-1β secretion, the three candidate compounds we examined may exert anti-inflammatory effects in treating human inflammatory diseases.

However, there were still some limitations as well in our study. We adopted a rat AM cell line for the in vitro experiments, but it is unclear whether the results can be extrapolated to humans. As a result, additional research on C/EBPβ in animal models would enhance our understanding of the many pathways behind lung injury, with promising implications for clinical medication development and usage. In addition, neither in vivo nor in vitro investigations were conducted to show further the inhibitory effect of the three candidate compounds on C/EBPβ/NOD2/RIPK2/IL-1β or their anti-inflammatory activity. As a result, our follow-up efforts must focus on addressing these deficiencies.

Conclusion

Our findings describe a novel function of C/EBPβ in regulating the transcription and secretion of the inflammatory cytokine IL-1β through the NOD2/RIPK2/NF-κB signaling pathway. In addition, three novel C/EBPβ inhibitors (N-caffeoyltryptophan, orilotimod, and petasiphenone) were identified with a more stable binding conformation and better pharmacokinetic parameters compared to helenalin.

Abbreviations

AMs, alveolar macrophages; MDP, muramyl dipeptide; DEGs, differentially expressed genes; iNOS, inducible nitric oxide synthase; C/EBPβ, CCAAT enhancer binding protein β; LPS, lipopolysaccharide; KEGG, Kyoto Encyclopedia of Genes and Genomes; GO, Gene Ontology; GSEA, Gene Set Enrichment Analysis; NLRs, NOD-like receptors; ILs, interleukins; ADME, absorption, distribution, metabolism, and excretion; MMP12, matrix metalloproteinase 12; AIM2, absent in melanoma 2; BBB, blood-brain barrier; CYP2D6, cytochrome P450 2D6; PPB, plasma protein binding levels; PAMPs, pathogen-associated molecular patterns; CXCL2, chemokine (C-X-C motif) ligand 2.

Data Sharing Statement

The data presented in this study are available in article.

Funding

This study was supported by National Key R&D Program of China (NO. 2019YFE0119300) and National Natural Science Foundation of China (NO. 82074158 and 82104594).

Disclosure

The authors declare no conflict of interest.

References

1. Balhara J, Gounni AS. The alveolar macrophages in asthma: a double-edged sword. *Mucosal Immunol*. 2012;5(6):605–609. doi:10.1038/mi.2012.74
2. Allard B, Panariti A, Martin JG. Alveolar macrophages in the resolution of inflammation, tissue repair, and tolerance to infection. *Front Immunol*. 2018;9:1777. doi:10.3389/fimmu.2018.01777
3. Hou F, Xiao K, Tang L, Xie L. Diversity of macrophages in lung homeostasis and diseases. *Front Immunol*. 2021;12:753940. doi:10.3389/fimmu.2021.753940
4. Lu HL, Huang XY, Luo YF, Tan WP, Chen PF, Guo YB. Activation of M1 macrophages plays a critical role in the initiation of acute lung injury. *Biosci Rep*. 2018;38(2):BSR20171555. doi:10.1042/BSR20171555
5. Akira S, Isshiki H, Sugita T, et al. A nuclear factor for IL-6 expression (NF-IL6) is a member of a C/EBP family. *EMBO J*. 1990;9(6):1897–1906. doi:10.1002/j.1460-2075.1990.tb08316.x
6. Zhang R, Li X, Liu Z, Wang Y, Zhang H, Xu H. EZH2 inhibitors-mediated epigenetic reactivation of FOSB inhibits triple-negative breast cancer progress. *Cancer Cell Int*. 2020;20:175. doi:10.1186/s12935-020-01260-5
7. Ikeda R, Nishida T, Watanabe F, et al. Involvement of CCAAT/enhancer binding protein-beta (C/EBPbeta) in epigenetic regulation of mouse methionine adenosyltransferase 1A gene expression. *Int J Biochem Cell Biol*. 2008;40(9):1956–1969. doi:10.1016/j.biocel.2008.02.004
8. Tang X, Liang Y, Sun G, He Q, Qu H, Gao P. UBQLN4 is activated by C/EBPβ and exerts oncogenic effects on colorectal cancer via the Wnt/β-catenin signaling pathway. *Cell Death Discov*. 2021;7(1):398. doi:10.1038/s41420-021-00795-4
9. Xu J, Liu L, Gan L, et al. Berberine acts on C/EBPβ/lncRNA Gas5/miR-18a-5p loop to decrease the mitochondrial ROS generation in HK-2 cells. *Front Endocrinol (Lausanne)*. 2021;12:675834. doi:10.3389/fendo.2021.675834
10. Dai XG, Li Q, Li T, et al. The interaction between C/EBPβ and TFAM promotes acute kidney injury via regulating NLRP3 inflammasome-mediated pyroptosis. *Mol Immunol*. 2020;127:136–145. doi:10.1016/j.molimm.2020.08.023
11. Lee JH, Sung JY, Choi EK, et al. C/EBPβ is a transcriptional regulator of Wee1 at the G_2/M phase of the cell cycle. *Cells*. 2019;8(2):145. doi:10.3390/cells8020145
12. Berberich-Siebelt F, Berberich I, Andrulis M, et al. SUMOylation interferes with CCAAT/enhancer-binding protein beta-mediated c-myc repression, but not IL-4 activation in T cells. *J Immunol*. 2006;176(8):4843–4851. doi:10.4049/jimmunol.176.8.4843
13. Matsuda T, Kido Y, Asahara S, et al. Ablation of C/EBPbeta alleviates ER stress and pancreatic beta cell failure through the GRP78 chaperone in mice. *J Clin Invest*. 2010;120(1):115–126. doi:10.1172/JCI39721
14. Chen X, Liu W, Ambrosino C, et al. Impaired generation of bone marrow B lymphocytes in mice deficient in C/EBPbeta. *Blood*. 1997;90(1):156–164.
15. Veremeyko T, Yung A, Anthony DC, Strekalova T, Ponomarev ED. Early growth response Gene-2 is essential for M1 and M2 macrophage activation and plasticity by modulation of the transcription factor CEBPβ. *Front Immunol*. 2018;9:2515. doi:10.3389/fimmu.2018.02515
16. Bersch KL, DeMeester KE, Zagani R, et al. Bacterial peptidoglycan fragments differentially regulate innate immune signaling. *ACS Cent Sci*. 2021;7(4):688–696. doi:10.1021/acscentsci.1c00200
17. Luo Y, Li Y, Ge P, Zhang K, Liu H, Jiang N. QKI-regulated alternative splicing events in cervical cancer: pivotal mechanism and potential therapeutic strategy. *DNA Cell Biol*. 2021;40(10):1261–1277. doi:10.1089/dna.2021.0069
18. Livak KJ, Schmittgen TD. Analysis of relative gene expression data using real-time quantitative PCR and the 2(-Delta Delta C(T)) method. *Methods*. 2001;25(4):402–408. doi:10.1006/meth.2001.1262
19. Sterling T, Irwin JJ. ZINC 15–Ligand discovery for everyone. *J Chem Inf Model*. 2015;55(11):2324–2337. doi:10.1021/acs.jcim.5b00559
20. Rao SN, Head MS, Kulkarni A, LaLonde JM. Validation studies of the site-directed docking program LibDock. *J Chem Inf Model*. 2007;47(6):2159–2171. doi:10.1021/ci6004299

21. Jakobs A, Steinmann S, Henrich SM, Schmidt TJ, Klempnauer KH. Helenalin acetate, a natural sesquiterpene lactone with anti-inflammatory and anti-cancer activity, disrupts the cooperation of CCAAT Box/Enhancer-binding Protein β (C/EBPβ) and co-activator p300. *J Biol Chem*. 2016;291 (50):26098–26108. doi:10.1074/jbc.M116.748129
22. Brooks BR, Brooks CL 3rd, Mackerell AD Jr, et al. CHARMM: the biomolecular simulation program. *J Comput Chem*. 2009;30(10):1545–1614. doi:10.1002/jcc.21287
23. Li H, Guo Z, Chen J, et al. Computational research of Belnacasan and new Caspase-1 inhibitor on cerebral ischemia reperfusion injury. *Aging*. 2022;14(4):1848–1864. doi:10.18632/aging.203907
24. Wang S, Chen Y, Hong W, Li B, Zhou Y, Ran P. Chronic exposure to biomass ambient particulate matter triggers alveolar macrophage polarization and activation in the rat lung. *J Cell Mol Med*. 2022;26(4):1156–1168. doi:10.1111/jcmm.17169
25. Wang W, Li X, Xu J. Exposure to cigarette smoke downregulates β2-adrenergic receptor expression and upregulates inflammation in alveolar macrophages. *Inhal Toxicol*. 2015;27(10):488–494. doi:10.3109/08958378.2015.1075628
26. Lee TJ, Choi YH, Song KS. The PDZ motif peptide of ZO-1 attenuates Pseudomonas aeruginosa LPS-induced airway inflammation. *Sci Rep*. 2020;10(1):19644. doi:10.1038/s41598-020-76883-9
27. Dai H, Pan L, Lin F, Ge W, Li W, He S. Mechanical ventilation modulates Toll-like receptors 2, 4, and 9 on alveolar macrophages in a ventilator-induced lung injury model. *J Thorac Dis*. 2015;7(4):616–624. doi:10.3978/j.issn.2072-1439.2015.02.10
28. Ge P, Luo Y, Okoye CS, et al. Intestinal barrier damage, systemic inflammatory response syndrome, and acute lung injury: a troublesome trio for acute pancreatitis. *Biomed Pharmacother*. 2020;132:110770. doi:10.1016/j.biopha.2020.110770
29. Huber R, Pietsch D, Panterodt T, Brand K. Regulation of C/EBPβ and resulting functions in cells of the monocytic lineage. *Cell Signal*. 2012;24 (6):1287–1296. doi:10.1016/j.cellsig.2012.02.007
30. Tanaka T, Akira S, Yoshida K, et al. Targeted disruption of the NF-IL6 gene discloses its essential role in bacteria killing and tumor cytotoxicity by macrophages. *Cell*. 1995;80(2):353–361. doi:10.1016/0092-8674(95)90418-2
31. Feng Y, Li M, Yangzhong X, et al. Pyroptosis in inflammation-related respiratory disease. *J Physiol Biochem*. 2022. doi:10.1007/s13105-022-00909-1
32. Dughbaj MA, Jayne JG, Park A, et al. Anti-inflammatory effects of RTD-1 in a murine model of chronic pseudomonas aeruginosa lung infection: inhibition of NF-κB, inflammasome gene expression, and Pro-IL-1β biosynthesis. *Antibiotics*. 2021;10(9). doi:10.3390/antibiotics10091043
33. Trachalaki A, Tsitoura E, Mastrodimou S, et al. Enhanced IL-1β release following NLRP3 and AIM2 inflammasome stimulation is linked to mtROS in airway macrophages in pulmonary fibrosis. *Front Immunol*. 2021;12:661811. doi:10.3389/fimmu.2021.661811
34. Zhang S, Fan Y, Qin L, et al. IL-1β augments TGF-β inducing epithelial-mesenchymal transition of epithelial cells and associates with poor pulmonary function improvement in neutrophilic asthmatics. *Respir Res*. 2021;22(1):216. doi:10.1186/s12931-021-01808-7
35. Xu X, Liu X, Dong X, Qiu H, Yang Y, Liu L. Secretory autophagosomes from alveolar macrophages exacerbate acute respiratory distress syndrome by releasing IL-1β. *J Inflamm Res*. 2022;15:127–140. doi:10.2147/JIR.S344857
36. Ma J, Yang X, Chen X. C/EBPβ is a key transcription factor of ox-LDL inducing THP-1 cells to release multiple pro-inflammatory cytokines. *Inflamm Res*. 2021;70(10–12):1191–1199. doi:10.1007/s00011-021-01509-3
37. Zhang HW, Wang Q, Mei HX, et al. RvD1 ameliorates LPS-induced acute lung injury via the suppression of neutrophil infiltration by reducing CXCL2 expression and release from resident alveolar macrophages. *Int Immunopharmacol*. 2019;76:105877. doi:10.1016/j.intimp.2019.105877
38. Xu-Vanpala S, Deerhake ME, Wheaton JD, et al. Functional heterogeneity of alveolar macrophage population based on expression of CXCL2. *Sci Immunol*. 2020;5(50):eaba7350. doi:10.1126/sciimmunol.aba7350
39. Zhang H, Luo J, Alcorn JF, et al. AIM2 inflammasome is critical for influenza-induced lung injury and mortality. *J Immunol*. 2017;198 (11):4383–4393. doi:10.4049/jimmunol.1600714
40. Niu Y, Yang S, Hu X. Activation of canonical inflammasome complex by acute silica exposure in experimental rat model. *Toxicol Res (Camb)*. 2022;11(1):162–168. doi:10.1093/toxres/tfab127
41. Chou WC, Rampanelli E, Li X, Ting JP. Impact of intracellular innate immune receptors on immunometabolism. *Cell Mol Immunol*. 2022;19 (3):337–351. doi:10.1038/s41423-021-00780-y
42. Samanta J, Singh S, Arora S, et al. Cytokine profile in prediction of acute lung injury in patients with acute pancreatitis. *Pancreatology*. 2018;18 (8):878–884. doi:10.1016/j.pan.2018.10.006
43. Wang SX, Abramson SB, Attur M, et al. Safety, tolerability, and pharmacodynamics of an anti-interleukin-1α/β dual variable domain immunoglobulin in patients with osteoarthritis of the knee: a randomized Phase 1 study. *Osteoarthritis Cartilage*. 2017;25(12):1952–1961. doi:10.1016/j.joca.2017.09.007
44. Zhou Y, Wang C, Lan X, Li H, Chao Z, Ning Y. Plasma inflammatory cytokines and treatment-resistant depression with comorbid pain: improvement by ketamine. *J Neuroinflammation*. 2021;18(1):200. doi:10.1186/s12974-021-02245-5
45. Vergis N, Patel V, Bogdanowicz K, et al. IL-1 Signal Inhibition In Alcoholic Hepatitis (ISAIAH): a study protocol for a multicentre, randomised, placebo-controlled trial to explore the potential benefits of canakinumab in the treatment of alcoholic hepatitis. *Trials*. 2021;22(1):792. doi:10.1186/s13063-021-05719-2